

Malonyl-CoA Synthetase, Encoded by *ACYL ACTIVATING ENZYME13*, Is Essential for Growth and Development of *Arabidopsis*

Hui Chen,¹ Hyun Uk Kim,² Hua Weng,³ and John Browse⁴

Institute of Biological Chemistry, Washington State University, Pullman, Washington 99164-6340

Malonyl-CoA is the precursor for fatty acid synthesis and elongation. It is also one of the building blocks for the biosynthesis of some phytoalexins, flavonoids, and many malonylated compounds. In plants as well as in animals, malonyl-CoA is almost exclusively derived from acetyl-CoA by acetyl-CoA carboxylase (EC 6.4.1.2). However, previous studies have suggested that malonyl-CoA may also be made directly from malonic acid by malonyl-CoA synthetase (EC 6.2.1.14). Here, we report the cloning of a eukaryotic malonyl-CoA synthetase gene, *Acyl Activating Enzyme13* (*AEE13*; At3g16170), from *Arabidopsis thaliana*. Recombinant *AEE13* protein showed high activity against malonic acid ($K_m = 529.4 \pm 98.5 \mu\text{M}$; $V_m = 24.0 \pm 2.7 \mu\text{mol/mg/min}$) but little or no activity against other dicarboxylic or fatty acids tested. Exogenous malonic acid was toxic to *Arabidopsis* seedlings and caused accumulation of malonic and succinic acids in the seedlings. *ae13* null mutants also grew poorly and accumulated malonic and succinic acids. These defects were complemented by an *AEE13* transgene or by a bacterial malonyl-CoA synthetase gene under control of the *AEE13* promoter. Our results demonstrate that the malonyl-CoA synthetase encoded by *AEE13* is essential for healthy growth and development, probably because it is required for the detoxification of malonate.

INTRODUCTION

CoA is an essential participant in a wide range of primary and secondary metabolic pathways that supply the core building blocks and energy for the cell. It is estimated that ~4% of enzymes use CoA as a cofactor or act on CoA-linked substrates (Begley et al., 2001). Acyl-CoA synthetase catalyzes the conversion of a carboxylic acid to its acyl-CoA thioester through an ATP-dependent two-step reaction. In the first step, the free fatty acid is converted to an acyl-AMP intermediate with the release of pyrophosphate. In the second step, the activated acyl group is coupled to the thiol group of CoA, releasing AMP and the acyl-CoA product (Groot et al., 1976). Acyl-CoA synthetase and some related proteins are characterized by a highly conserved 12-amino acid sequence that forms the core of an AMP binding motif (PROSITE PS00455). Based upon this conserved sequence signature, we have identified a family of 44 genes in *Arabidopsis*

thaliana that encode acyl-activating enzymes (AAEs) (Shockey et al., 2003). Currently, about half of the 44 AAE proteins have known biochemical functions.

Malonyl-CoA is the precursor for the de novo synthesis and elongation of fatty acids (Baud et al., 2003, 2004) as well as the formation of flavonoids, isoflavonoids, stilbenoids (Peer et al., 2001), and many malonylated compounds, including malonylated 1-aminocyclopropane-1-carboxylic acid, D-amino acids, and flavonoid glycosides (Liu et al., 1984; Taguchi et al., 2010). In eukaryotic cells, it has been generally accepted that malonyl-CoA is formed almost exclusively by acetyl-CoA carboxylase (ACCase; EC 6.4.1.2) that catalyzes the ATP-dependent formation of malonyl-CoA from acetyl-CoA and bicarbonate. Two forms of ACCase have been identified in plants: a multifunctional homodimeric form, found in the cytosol of all plants and the plastids of monocots, and a multisubunit heteromeric form in the plastids of dicots (Ohlrogge and Browse, 1995; Fatland et al., 2005). The plastidic pool of malonyl-CoA contributes to de novo fatty acid synthesis, whereas the cytosolic pool of malonyl-CoA is used for various biosynthetic pathways, including fatty acid elongation (Baud et al., 2003).

Malonic acid, a homolog of succinic acid, has been used in biochemical research as a competitive inhibitor of succinate dehydrogenase in the tricarboxylic acid cycle (Quastel and Wooldridge, 1928; Greene and Greenamyre, 1995). However, little information is available regarding the synthesis and function of malonate in biological systems, although it is present at measurable concentrations in some tissues of plants and animals. In animals, a considerable amount of malonic acid was detected in rat brain (Mitzen and Koeppen, 1984). Turner and Hartman (1925) first reported its presence in the leaves of alfalfa (*Medicago sativa*). Later, it was found in wheat (*Triticum aestivum*), tobacco (*Nicotiana tabacum*), and ~18 species of

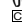
¹ Current address: Donald Danforth Plant Science Center, 975 N. Warson Rd., St. Louis, MO 63132.

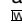
² Current address: Department of Agricultural Bioresources, National Academy of Agricultural Sciences, 225 Seodun-Dong, Suwon 441-707, Republic of Korea.

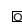
³ Current address: Department of Horticulture and Landscape Architecture, 635 Agricultural Mall Drive, Purdue University, West Lafayette, IN 47907-2010.

⁴ Address correspondence to jab@wsu.edu.

The author responsible for distribution of materials integral to the findings presented in this article in accordance with the policy described in the Instructions for Authors (www.plantcell.org) is: John Browse (jab@wsu.edu).

 Some figures in this article are displayed in color online but in black and white in the print edition.

 Online version contains Web-only data.

 Open Access articles can be viewed online without a subscription. www.plantcell.org/cgi/doi/10.1105/tpc.111.086140

leguminous plants (Nelson and Hasselbring, 1931; Bentley, 1952; Bellin and Smeby, 1958). In the roots and nodules of some legumes, malonate accounts for as much as 4% of the dry weight (Li and Copeland, 2000), and it has been suggested to have a role in carbon and nitrogen exchange during symbiotic nitrogen fixation (Kim, 2002).

Despite extensive research on malonyl-CoA production by ACCase and its regulation, evidence is available in the literature showing that malonyl-CoA can also be made directly from malonic acid by malonyl-CoA synthetase (EC 6.2.1.14). Gueguen et al. (2000) detected malonyl-CoA synthetase activity in the soluble fraction of mitochondria isolated from pea (*Pisum sativum*) leaves, and Koeppen et al. (1974) reported activity in mitochondria from rat brain. However, the importance and physiological function of these enzymes in biological systems are unknown, and the genes encoding these proteins have not been identified to date.

Many bacteria are able to grow on malonate as sole source of carbon and energy (Dimroth and Hilbi, 1997). Hayaishi (1955) found malonate was activated to malonyl-CoA and then malonyl-CoA was decarboxylated to form acetyl-CoA and CO₂ in *Pseudomonas fluorescens* adapted to malonate. The genes encoding malonyl-CoA synthetase (MatB) have been cloned from symbiotic bacteria *Rhizobium trifolii* (An and Kim, 1998) and *Bradyrhizobium japonicum* that develop symbioses with legumes (Koo and Kim, 2000). In *R. trifolii*, the *matB* gene is part of the *matABC* operon, with *matA* encoding a malonyl-CoA decarboxylase and *matC* encoding a putative dicarboxylate carrier protein. It has been suggested that these three proteins are involved in the uptake of malonate from the legume host and its subsequent conversion to acetyl-CoA in the bacteroids (An and Kim, 1998).

Here, we report the identification of a eukaryotic gene encoding malonyl-CoA synthetase, the *ACYL ACTIVATING ENZYME13* (*AAE13*) gene of *Arabidopsis*. We also show that the human *AAE13* homolog, Acyl-CoA Synthetase Family Member 3 (ACSF3), is a malonyl-CoA synthetase. Exogenous malonic acid poisoned growth of wild-type *Arabidopsis* seedlings and led to accumulation of succinate. *aae13* mutant plants accumulated both malonate and succinate and were severely compromised in growth, development, and fecundity. These results indicate that malonyl-CoA synthetase encoded by *AAE13* is required to metabolize free malonate and prevent its accumulation to levels that are toxic to cell metabolism and plant growth.

RESULTS

AAE13 Encodes a Malonyl-CoA Synthetase

As part of a genomics project to investigate *Arabidopsis* genes that encode putative CoA synthetase enzymes (Shockey et al., 2003), we have tested individual recombinant proteins for acyl-CoA synthetase activity against ~100 different carboxylic acids using a spectrophotometer-based coupled enzyme assay or an HPLC-based enzyme assay, as described in Methods. In this process, a full-length cDNA of *AAE13* was obtained by RT-PCR from *Arabidopsis* and expressed as a His fusion protein in *Escherichia coli* using the pDEST17 vector (Invitrogen). Expression of His-*AAE13* was induced by addition of L-arabinose, and

the recombinant protein was purified by nickel column affinity chromatography (Figure 1A). During biochemical screening, *AAE13* was found to have a high activity against malonic acid (Figures 1B and 1C), converting it efficiently to malonyl-CoA. As shown in Figure 1B, in the control containing boiled enzyme, free CoA has a retention time of 10.9 min and an absorbance maximum at 257.5 nm (peak 1). In assays containing the purified His-*AAE13* protein, a new peak corresponding to malonyl-CoA was formed (peak 2, retention time 11.6 min). This was identified as malonyl-CoA by its coelution with a malonyl-CoA standard and by its UV absorbance spectrum, which was identical to that of the standard, with an absorption maximum at 256.3 nm.

Additional assays demonstrated that the pH dependency of malonyl-CoA synthetase activity showed a relatively broad optimum of pH 6.5 to 8.0 for the recombinant *AAE13* protein (Figure 1D). At pH 7.5 and with saturating concentrations of CoA (0.5 mM) and ATP (5 mM), the purified *AAE13* protein exhibited Michaelis-Menten kinetics with respect to malonate concentration, providing a calculated V_{\max} of 24.0 ± 2.7 (SD) $\mu\text{mol}/\text{min}/\text{mg}$ protein and a K_m of 529.4 ± 98.5 μM (Figure 1E).

As shown in Table 1, *AAE13* was specific for malonic acid. Its activity against 2-methylmalonic acid was only 12% of that against malonic acid, and it had no activity against other dicarboxylic acids, such as 2-hydroxymalonic acid (tartronic acid), oxalic acid, succinic acid, glutaric acid, adipic acid, and pimelic acid. In addition, it showed no activity against short-, medium-, and long-chain carboxylic acids ranging from acetic acid to octadecanoic acid.

Most malonyl-CoA synthetases so far characterized have relatively high K_m values in the range of several hundred micromoles (Table 2). The K_m of the *Arabidopsis* enzyme is 10-fold lower than that reported for the enzyme of pea leaf mitochondria and is comparable to the K_m values for several bacterial enzymes. The V_{\max} for the purified *AAE13* protein is also comparable to those of malonyl-CoA synthetases from bacteria, except for the low-activity enzyme from *P. fluorescens*.

AAE13 cDNA was predicted to encode a 544-amino acid protein having a calculated molecular mass of 60,062 and an isoelectric point of 5.95. However, as shown in Figure 1A, the apparent molecular mass of the His-tagged *AAE13* was ~67.9 kD as determined by SDS-PAGE, which is several kilodaltons higher than the calculated value. The reasons for this inconsistency are unknown, but in some cases, proteins resistant to the treatments of high temperature and SDS may give higher apparent molecular masses (Mirecka et al., 2006).

AAE13 Is the Founding Member of a Novel Phylogenetic Clade of the Eukaryotic AAE Superfamily

Although malonyl-CoA synthetase activities have been described from bacteria, plants, and animals (Table 2), so far, only two genes from prokaryotes have been cloned and shown to encode malonyl-CoA synthetases. These are the *MatB* genes from the symbiotic nitrogen fixing bacteria *R. trifolii* (An and Kim, 1998) and *B. japonicum* (Koo and Kim, 2000). From the HomoloGene database at the National Center for Biotechnology Information (<http://www.ncbi.nlm.nih.gov/homologene/?term=aae13>), we identified 10 homologs of *AAE13*. These include human ACSF3

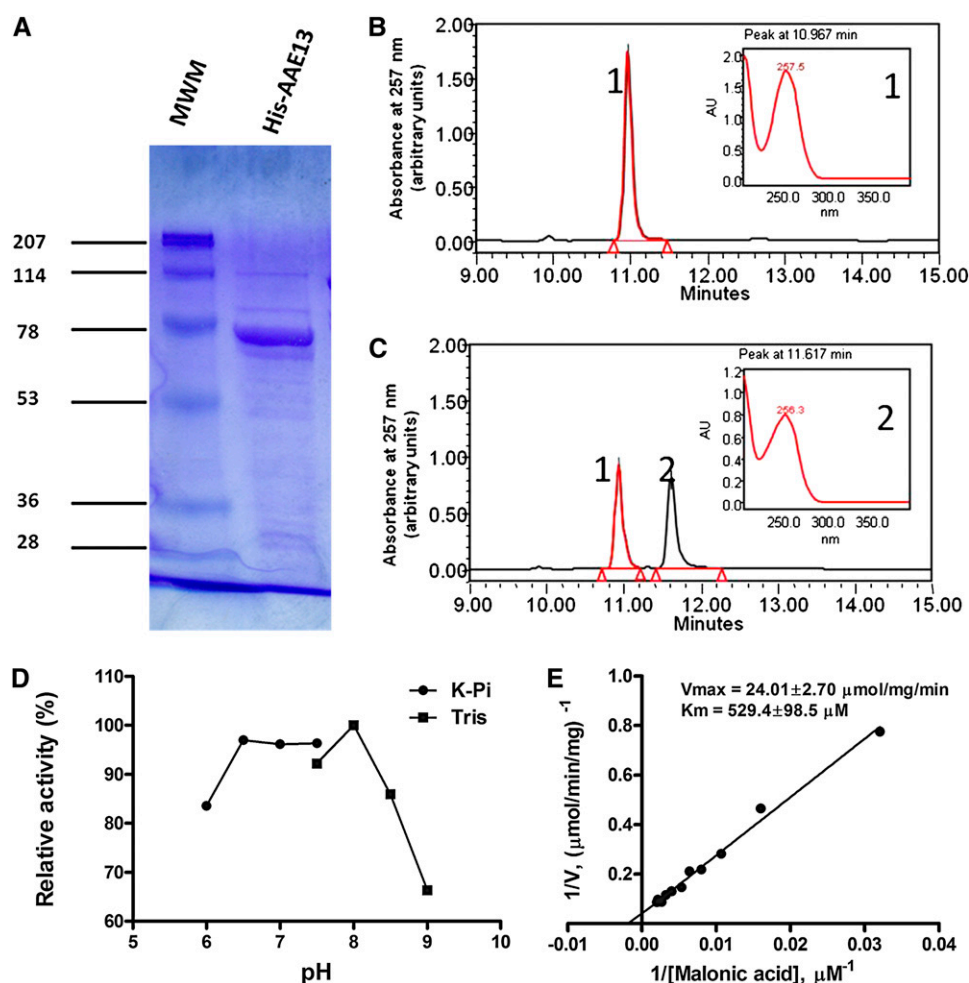


Figure 1. Biochemical Characterization of Recombinant AAE13 Protein.

(A) SDS-PAGE gel with Coomassie blue–stained His-AAE13 protein, following purification by nickel-affinity chromatography. Size of molecular mass markers (MWM; kD) are indicated at left.

(B) and **(C)** HPLC-based assay for malonyl-CoA synthetase activity of recombinant His-AAE13. The control in **(B)** contained boiled enzyme. Peak 1 is free CoA with absorption peak at 257.5 nm (inset). Active enzyme in **(C)** produces malonyl-CoA (peak 2) with absorption peak at 256.3 (inset). Assays were incubated for 10 min as described in Methods.

(D) The optimum pH for His-AAE13 against malonic acid; 200 mM potassium phosphate buffer at pH 6.0 to 7.5 and 100 mM Tris-HCl buffer at pH 7.5 to 9.0 were used. The experiment was repeated twice with similar results.

(E) Kinetic analysis of AAE13 activity with malonic acid. For the determination of K_m and V_{max} , the malonic acid concentration in the assay mixtures varied between 62.5 and 625 μM . Experiments were performed at least in triplicate. Values for K_m and V_{max} were obtained by nonlinear regression to the Michaelis-Menten equation.

[See online article for color version of this figure.]

and homologs from chimpanzee, rat, mouse, cow, chicken, and zebra fish. Additional homologs include one from rice and two fungal proteins from rice blast fungus (*Magnaporthe grisea*) and bread mold (*Neurospora crassa*).

To test whether or not members of the ACSF3-related group have malonyl-CoA synthetase activity, we cloned the full-length human ACSF3 cDNA (GenBank accession number NP_777577) into the pDEST17 vector. The resulting plasmid, pDEST17-ACSF3, was expressed in *E. coli* strain BL21AI-competent cells, but the His-ACSF3 protein was in an insoluble form. We then

cloned the human ACSF3 cDNA into the pRMG-nMAL vector so that ACSF3 would be expressed as a fusion with maltose binding protein as well as hexa-histidine (His6) tag (Thines et al., 2007). By this means, a MBP-ACSF3-His6 protein was successfully expressed in a soluble form in BL21AI cells and partially purified by nickel column affinity chromatography (see Supplemental Figure 1A online). ACSF3 cDNA was predicted to encode a 576-amino acid protein having a calculated molecular mass of 64,130 and an isoelectric point of 8.37. Since the size of MBP is ~ 40 kD, the MBP-ACSF3-His fusion protein had a calculated molecular

Table 1. Substrate Specificity of AAE13

Substrate	Structure	Relative Activity (%)
Malonic acid	HOOC-CH ₂ -COOH	100
2-Methylmalonic acid	HOOC-CHCH ₃ -COOH	11.7
Tartronic acid	HOOC-CHOH-COOH	<1
Monomethyl malonate	CH ₃ OOC-CH ₂ -COOH	<1
Succinic acid	HOOC(CH ₂) ₂ COOH	<1
Glutaric acid	HOOC(CH ₂) ₃ COOH	<1
Adipic acid	HOOC(CH ₂) ₄ COOH	<1

CoA synthetase activities were determined by HPLC with a substrate concentration of 5.0 mM.

mass of ~105 kD, which was in agreement with its apparent molecular mass as determined by SDS-PAGE (see Supplemental Figure 1A online).

The recombinant human ACSF3 protein indeed had malonyl-CoA synthetase activity as determined by the coupled-enzyme spectrophotometric assay as well as by our HPLC-based assay. Control assays containing crude lysate or eluate from the Ni-nitriloacetic acid column from cultures expressing the MBP-His6 protein did not provide any detectable malonyl-CoA synthetase activity. In contrast with the AAE13 protein, the pH dependency of the human enzyme showed a relatively narrow optimum at pH9 (see Supplemental Figure 1B online). Assays conducted at this pH demonstrated Michaelis-Menten kinetics for the enzymes with a K_m for malonate of 0.66 ± 0.10 mM and a V_{max} of 2.5 ± 0.8 μ mol/min/mg protein. The difference in V_{max} between ACSF3 and AAE13 may be partly due to the lower level of protein purification (see Supplemental Figure 1A online) and possibly destabilization of the protein by fusion to MBP. Like its plant counterpart, ACSF3 was also specific for malonic acid. ACSF3 is expressed in many tissues and organs (see Supplemental Table 1 online) with high expression in blood, lymph, thymus, and tonsil tissues.

Subcellular Localization of AAE13

The amino acid sequence alignment of four characterized malonyl-CoA synthetase proteins, AAE13, ACSF3, and two MatB proteins, is shown in Figure 2. Overall, these four proteins have 26.7% sequence identity and 76.8% sequence similarity. The underlined sequence is the conserved 12-amino acid AMP binding motif (PS00455). In contrast with the other three proteins,

ACSF3 had an additional N-terminal sequence of 28 amino acids (Figure 2). A program for estimating subcellular localization of proteins, TargetP (Emanuelsson et al., 2000), predicted ACSF3 to be localized to the mitochondria with a score of 0.925 and the highest reliability class value of 1. This result is in agreement with the mitochondrial localization of malonyl-CoA synthetase activity in rat brain (Koeppen et al., 1974).

By contrast, predictions of subcellular localization of AAE13 using TargetP and WoLF PSORT (Horton et al., 2006) indicated the cytosol and nucleus as possible sites, but with low reliability scores. There is no identifiable nuclear targeting motif in AAE13. To study the subcellular localization of AAE13 experimentally, we generated in-frame fusions of the *AAE13* cDNA with a sequence encoding green fluorescent protein (GFP) and expressed them in *Arabidopsis* mesophyll protoplasts under control of the 35S promoter. Figure 3A shows the GFP signal from protoplasts transfected with the *Pro35S:AAE13-GFP* and *Pro35S:GFP-AAE13* constructs. In both cases, the green fluorescence is visible in the cytoplasm around the cell periphery. It is not found in the chloroplasts (shown by red chlorophyll autofluorescence) but is seen in the optical section through the nucleus. This distribution of green fluorescence is similar to that seen in protoplasts expressing the GFP protein, which is known to localize to the cytoplasm and nucleus. In addition, expression of *Pro35S:AAE13-GFP* transiently in *Nicotiana benthamiana* leaves and stably in transgenic *Arabidopsis* plants indicated localization to the nucleus as well as the cytoplasm (see Supplemental Figure 2 online). Although expression of AAE13-GFP fusion proteins provided consistent results, additional experimental approaches will be required to test the possibility of nuclear localization of AAE13.

Malonyl-CoA Synthetase Activity and Malonic Acid in *Arabidopsis* Tissues

Our results indicate that AAE13 is a malonyl-CoA synthetase in vitro. However, to the best of our knowledge, neither malonyl-CoA synthetase activity nor its substrate, malonic acid, has been reported in *Arabidopsis* before. To address this question, we first assayed the malonyl-CoA synthetase activity in the crude extracts of different *Arabidopsis* tissues. As shown in Figure 3B, malonyl-CoA synthetase activities were detected in all of the *Arabidopsis* tissues examined. The highest activity was found in flowers, and this result is consistent with the expression pattern of *AAE13* in various *Arabidopsis* tissues

Table 2. Comparison of Malonyl-CoA Synthetase Activities from Different Sources

Enzyme Source	K_m (mM)	V_{max} (μ mol/min/mg Protein)	Reference
<i>Arabidopsis</i>	0.530	24.000	This study
Pea leaf mitochondria	5.200	–	Gueguen et al. (2000)
<i>P. fluorescens</i>	0.380	0.117	Kim and Bang (1985)
<i>Rhizobium japonicum</i>	0.200	21.300	Kim and Chae (1991)
<i>R. trifolii</i>	0.217	18.980	Kim et al. (1993)
<i>B. japonicum</i>	0.260	22.700	Kim et al. (1993)
<i>Rattus norvegicus</i> (rat) brain mitochondria	0.080	–	Koeppen et al. (1974)

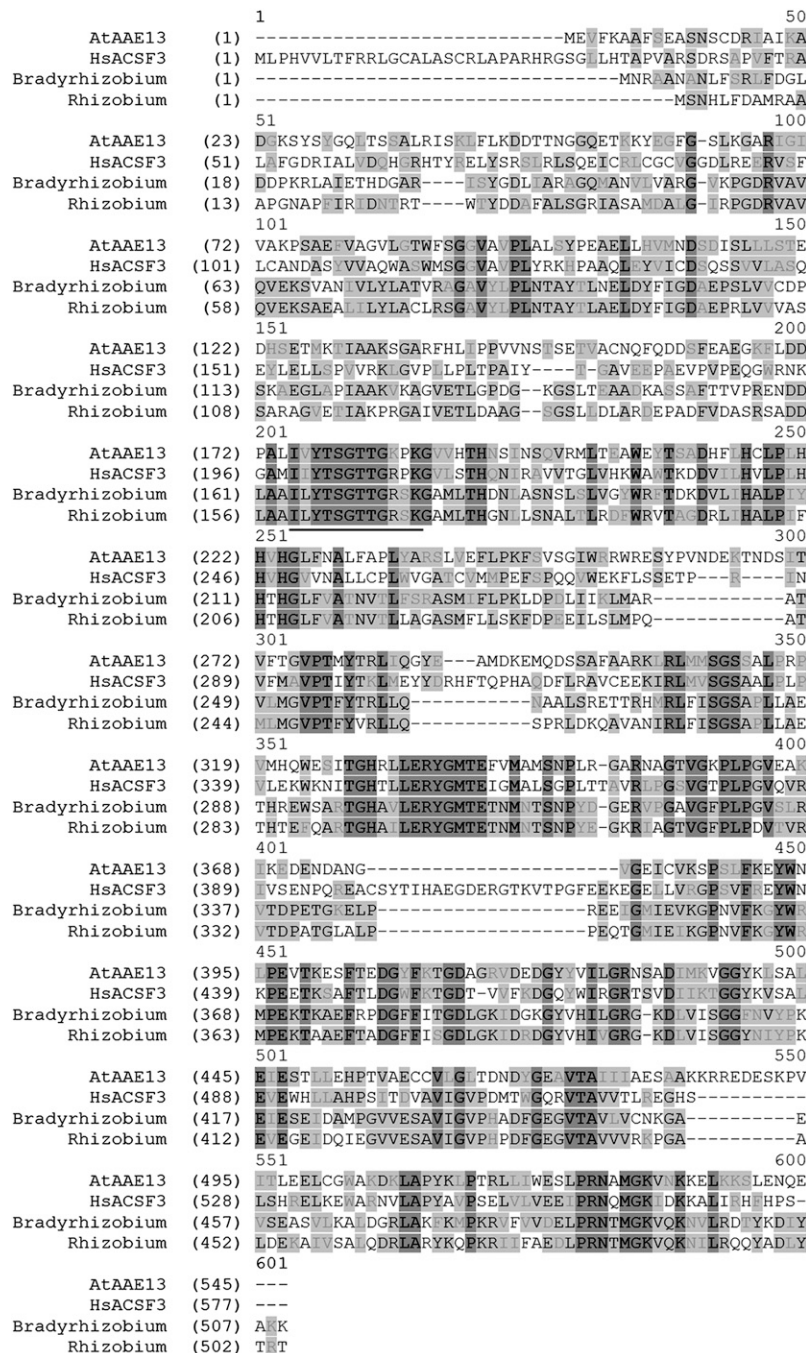


Figure 2. Alignment of Characterized AAE13 Homologs.

Malonyl-CoA synthetases from *Arabidopsis* (AtAAE13), human (HsACSF3), *B. japonicum* (Bradyrhizobium), and *Rhizobium leguminosarum* (Rhizobium) were aligned using Vector NTI. Dark-gray shading indicates identical residues; light-gray shading indicates conserved substitutions. The underlined sequence is the conserved 12-amino acid AMP binding motif (PS00455).

where the highest level of *AAE13* transcript was found in flowers (Shockey et al., 2003). Transcript profiling data for *AAE13* available in the AtGenExpress database (Schmid et al., 2005) confirmed the high expression in floral organs (Figure 3C) and indicated that *AAE13* is induced by dehydration (treatment

with 300 mM mannitol) and treatment with abscisic acid (ABA; see Supplemental Figure 3 online).

We then used a gas chromatography–mass spectrometry (GC-MS) method to profile the water-soluble constituents in the extracts of different *Arabidopsis* tissues. As shown in Figure

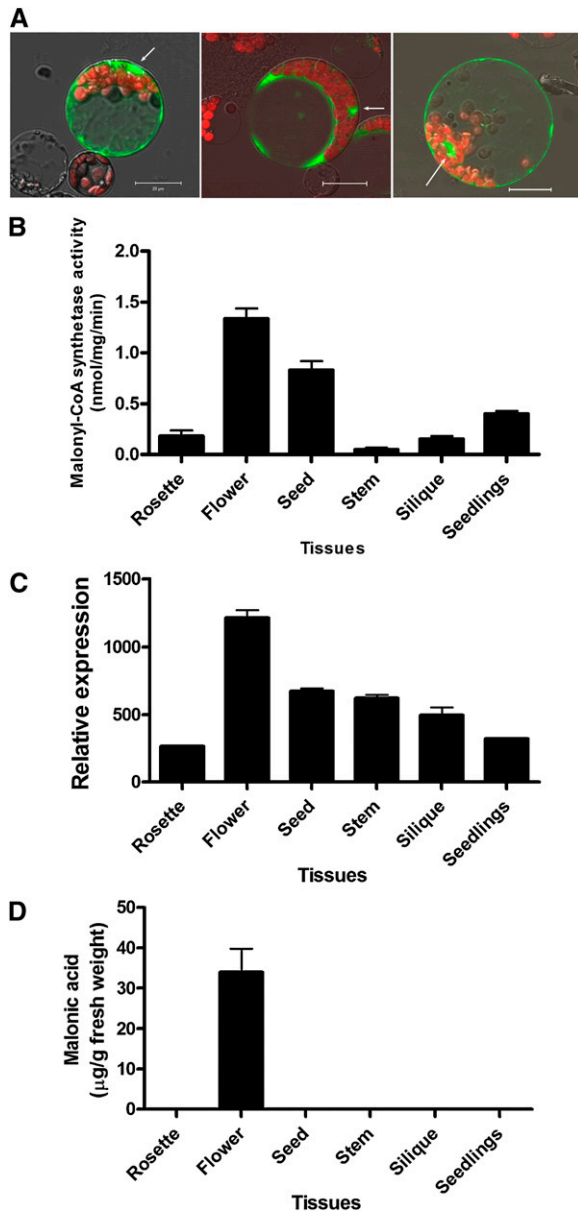


Figure 3. Expression and Activity of AAE13 in Wild-Type *Arabidopsis*.

(A) Subcellular localization of AAE13. *Arabidopsis* leaf-mesophyll protoplasts transfected with *Pro35S::GFP* (left), *Pro35S::GFP-AAE13* (center), or *Pro35S::AAE13-GFP* (right) constructs. Green fluorescence signals were observed using confocal microscopy with excitation at 488 nm and detection at 505 nm. (Arrows indicate nuclei; bars = 20 μm).

(B) Malonyl-CoA synthetase activities in different tissues of the wild type determined by the HPLC-based assay.

(C) Organ-specific expression data of *AAE13* retrieved from the Genevestigator database (www.genevestigator.ethz.ch/).

(D) Free malonic acid levels in different tissues of wild-type *Arabidopsis* as quantified by GC-MS. Values represent mean \pm SD ($n = 3$).

3D, *Arabidopsis* flowers contained a small but significant amount of malonic acid, whereas the levels of malonic acid in other tissues were below the detection limit ($\sim 2 \mu\text{g/g}$ fresh weight) of our analysis.

Exogenous Malonic Acid Is Toxic to *Arabidopsis*

Although we detected malonic acid in the flowers of *Arabidopsis* (Figure 3D), as a well-known competitive inhibitor of succinic acid dehydrogenase (Quastel and Wooldridge, 1928), it is potentially toxic to plants. To test the toxicity of malonic acid to *Arabidopsis*, we sowed wild-type *Arabidopsis* seeds on agar plates supplemented with different concentrations of malonic acid (0 to 10 mM). After 7 d of growth, we examined and analyzed these seedlings. As shown in Figure 4A, malonic acid at 1 mM in the medium did not show any visible toxicity to the seedlings. However, 5 mM malonic acid caused an easily observable inhibition of root and shoot growth, and on medium containing 10 mM malonic acid, growth inhibition was considerably more pronounced.

We harvested the shoots from these seedlings, rinsed them to remove any medium containing malonic acid, and used GC-MS to measure their levels of malonic acid and succinic acid (Figure 4B). Using this method, we were able to detect malonic acid (peak 1 in Figure 4B), succinic acid (peak 5), as well as Val, Pro, Gly, and glyceric acid (peaks 2, 3, 4, and 6, respectively). The identities of these compounds were confirmed by comparisons of retention times and mass spectra with authentic standards. As shown in Figure 4B, in control plants grown in the absence of malonic acid, neither malonic acid nor succinic acid was detectable in the seedling shoots, while glyceric acid and the amino acids are detected at $\sim 0.1 \text{ mg/g}$ fresh weight. By contrast, both malonic acid and succinic acid were detected in the shoots of plants grown on 5 mM malonic acid. The concentrations of glyceric acid, Val, and Gly were similar to control plants. The concentration of Pro was increased approximately threefold relative to the control.

We quantified the levels of malonic and succinic acids in the seedling shoots from the plates supplemented with different concentrations of malonic acid. When supplemented malonic acid was below 1 mM, concentrations that did not visibly compromise the growth of plants, almost no malonic acid or succinic acid was found in the shoots (Figures 4A and 4C). However, as the concentration of malonic acid in the medium was increased further, the accumulation of malonic acid and succinic acid in shoot tissue occurred concomitantly with the appearance of the toxic phenotype of seedlings (Figures 4A and 4C). In the plate supplemented with 5 mM malonic acid, the concentration at which a growth phenotype was first evident, the malonic acid and succinic acid levels in the shoots reached 250 and 66 $\mu\text{g/g}$ fresh weight, respectively.

Our experiments indicate that malonic acid can be taken up by roots and transported to the shoots resulting in the overaccumulation of succinic acid, presumably through the inhibition of succinic acid dehydrogenase in mitochondria. This result was similar to the previous observations with tobacco plant where malonic acid and succinic acid accumulated in the excised leaves cultured in solutions of malonic acid (Vickery, 1959).

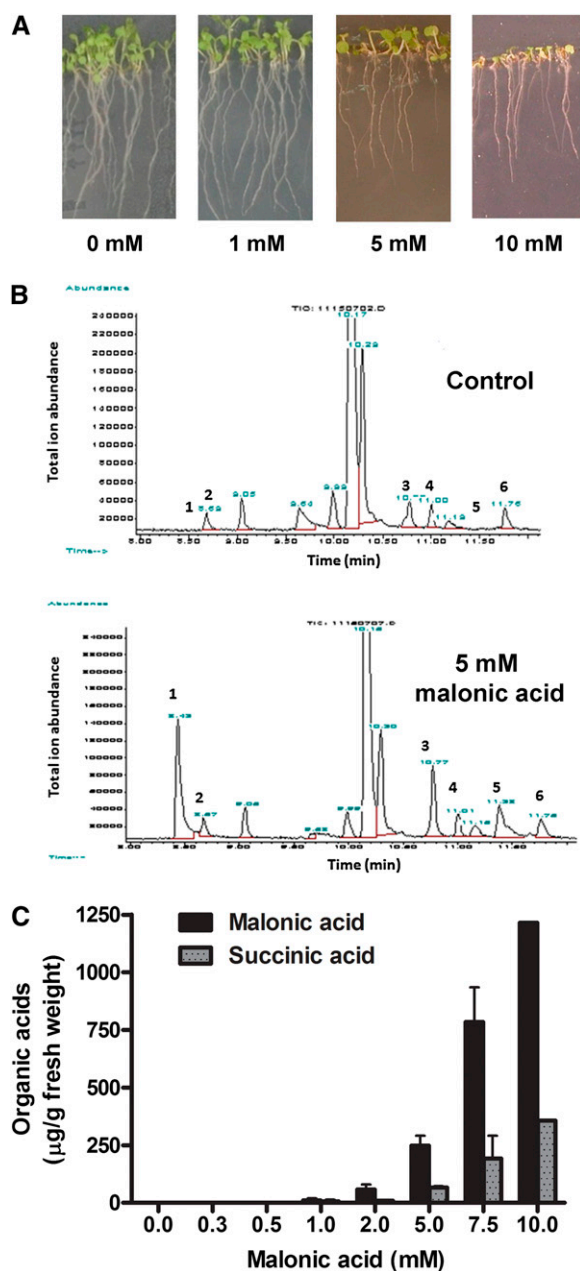


Figure 4. Effect of Malonic Acid on the Growth and Metabolism of *Arabidopsis* Seedlings.

(A) *Arabidopsis* seedlings grown on agar plates supplemented with different concentrations of malonic acid. The pictures were taken 7 d after germination.

(B) GC-MS chromatograms of water-soluble constituents extracted from shoots of seedlings grown without malonic acid (top) or with 5 mM malonic acid. Peaks 1 to 6 correspond to malonic acid, Val, Pro, Gly, succinic acid, and glyceric acid, respectively.

(C) Contents of malonic acid and succinic acid in the shoots of *Arabidopsis* seedlings grown on different concentrations of malonic acid. Data are means \pm SD ($n = 3$).

[See online article for color version of this figure.]

Compromised Growth and Development of an *aae13* Mutant

To assess the biological role of malonyl-CoA synthetase, we set out to identify a mutant in *aae13*. A T-DNA insertion line obtained from the ABRC at Ohio State University, SALK_083785 was cataloged to have a T-DNA insertion in the 12th exon of *AAE13* (Figure 5A). We initially grew 12 plants of this line and genotyped the plants by PCR using oligonucleotide primers, P1 and P2, flanking the reported T-DNA insertion site, together with a primer, LBa1, designed to the T-DNA left border. Ten of these plants were determined to be wild-type and two hemizygous for the T-DNA insertion; no homozygous mutant plants were identified. We therefore collected seeds from one of the hemizygous plants and designated the line *aae13-1*. Progeny seeds from this *AAE13/aae13-1* hemizygous plant were germinated on agar medium containing 1% Suc, and the seedlings were genotyped by PCR using the primers P1, P2, and LBa1. Of 55 seedlings analyzed, 15 plants contained only a 0.9-kb band corresponding to the expected P1-P2 fragment from wild-type DNA, 28 plants contained both the 0.9-kb band and a 0.4-kb band that corresponds to the size expected for the LBa1-P2 fragment, and 12 plants contained only the 0.4-kb band, indicating that these plants were homozygous for the *aae13-1* mutation (Figure 5B).

We isolated RNA from wild-type *Arabidopsis* and the *aae13-1* mutant and performed RT-PCR using the primers (P3 and P4) designed to amplify the *AAE13* open reading frame. A band at 1.6 kb, corresponding to the expected size of *AAE13* transcript, was obtained from wild-type RNA but not from RNA of the *aae13-1* homozygous mutant (Figure 5B). However, when the primers P3 and P5 were used for RT-PCR analysis, a RT-PCR product of 1.4 kb was detected in both samples (Figure 5B). This result suggested that T-DNA insertion may result in the generation of a truncated *AAE13* transcript in the *aae13-1* mutant, which might possibly be translated into a truncated *AAE13* protein.

To explore this possibility further, we amplified a DNA fragment from the genomic DNA of the *aae13-1* mutant using the P1 gene-specific primer and LBa1. The PCR product contained the sequence of the fusion region of *AAE13* and the T-DNA insertion. Sequencing data indicated that the fusion of *AAE13* and the T-DNA left border could produce a chimeric transcript containing the first 1389 bp of *AAE13* and sequence from the T-DNA that includes an in-frame translation stop codon after 49 bp. The amino acid sequences of the C terminus of wild-type *AAE13* and the protein encoded in the *aae13-1* mutant are shown in Figure 5C. The chimeric transcript was amplified from the *aae13-1* mutant by RT-PCR using the primers P3 and P6. As shown in Figure 5B, the 1.4-kb product was detected in the *aae13-1* mutant but not in the wild type. We cloned this chimeric cDNA gene into Gateway expression vector pDEST17 and expressed it in *E. coli* BL21AI cells. The His-tagged protein, purified from induced *E. coli* cultures, did not exhibit any detectable malonyl-CoA synthetase activity, suggesting that the function of *AAE13* requires its C-terminal domain and that *aae13-1* is a null mutant. These conclusions are consistent with the observation that the C terminus of *AAE13* is homologous to other malonyl-CoA synthetases and to the larger LuxE superfamily of proteins.

In the initial experiment with 55 progeny from a heterozygous plant, all of the wild-type and hemizygous plants showed normal

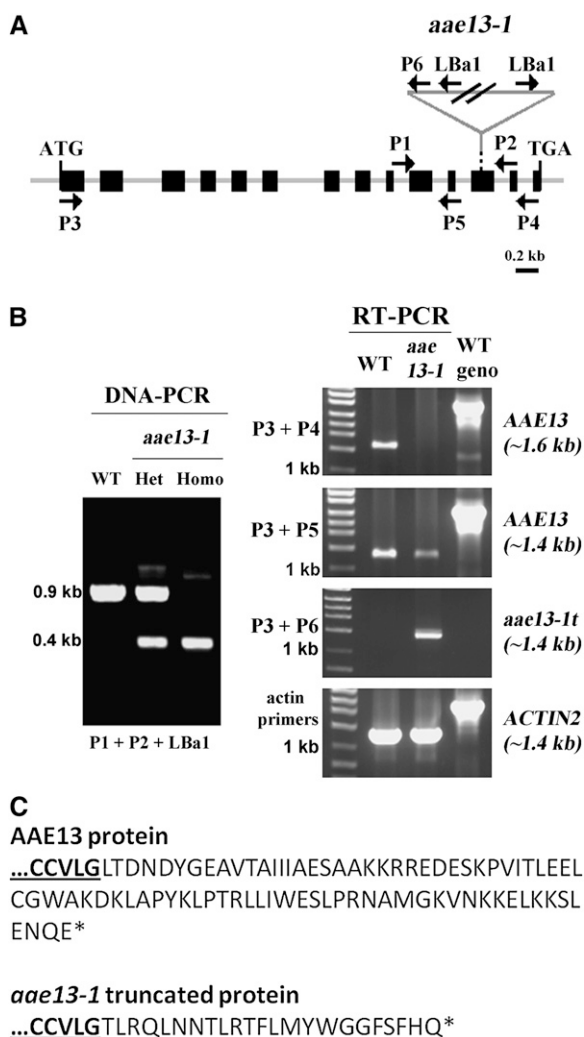


Figure 5. Molecular Characterization of the *aae13-1* Mutant.

(A) Diagram of the *aae13-1* locus, showing locations of the T-DNA insert and the primers used for analysis. Black boxes, exons; lines, introns.

(B) Identification of the mutant by genomic PCR using gene-specific primers, P1 and P2, and the T-DNA left border primer, LbA1 (left panel). RT-PCR (right panel) indicates that the *aae13-1* mutant lacks the full-length *AAE13* transcript, detected by P3+P4 and P3+P5, but contains a truncated and chimeric transcript detected by P3+P6. A repeat experiment gave similar results. Het, heterozygote; Homo, homozygote; WT, wild type; WT geno, wild-type genomic DNA.

(C) Comparison of the C-terminal amino acid sequence of *AAE13* with that of a truncated and chimeric *aae13-1* protein. The amino acid sequence in gray was derived from the T-DNA.

growth and development. However, all 12 of the homozygous mutant plants exhibited strong defects in growth and development. The segregation ratio (wild type:hemizygous:homozygous = 15:28:12) indicated that the small and sick phenotype segregated as a single, recessive mutation and cosegregated with the *aae13-1* T-DNA insertion.

As shown in Figure 6A, after 12 d on agar media, wild-type seedlings had produced five to six leaves, while *aae13-1* mutant

seedlings showed retarded growth with pale green cotyledons and limited leaf growth. At day 48, the wild-type plants had matured and produced seeds, whereas mutant plants remained as small compact rosettes. The *aae13-1* mutant was also severely compromised during growth on soil. As shown in Figure 6A, compared with the wild-type plants 23 d after sowing, *aae13-1* plants are small rosettes with chlorotic leaves. After 39 d growth, many of the mutant plants had died and the others remained small and chlorotic. Eventually, ~10% of the mutant plants bolted. Although flowers on these plants appeared similar to those on the wild type and produced at least some normal-looking pollen (Figure 6C), seed set was greatly reduced with only a low proportion of siliques containing any viable seed.

We used the GC-MS method to measure the tissue concentrations of malonic and succinic acids in extracts from the 12-d-old seedlings grown on agar plates. In the mutant, the levels of malonic acid and succinic acid were 180 and 50 $\mu\text{g/g}$ fresh weight (Figure 6D), respectively, which are comparable to those in wild-type seedlings grown on media containing 5 mM malonic acid (250 and 70 $\mu\text{g/g}$ fresh weight, respectively; Figure 4C).

Complementation of *aae13-1* Plants

The *MatB* gene from the symbiotic bacterium *B. japonicum* has been previously characterized as encoding a malonyl-CoA synthetase enzyme (Koo and Kim, 2000). To determine if this enzyme could complement the phenotype of *aae13-1*, we placed the *MatB* coding sequence under control of the *Arabidopsis AAE13* promoter as construct pBjMCS in a transformation vector containing the BASTA selectable marker. This vector was used to transform *AAE13/aae13-1* heterozygous plants. We used genomic PCR (Figure 7A) to analyze 48 T1 plants that were resistant to BASTA treatment and found that nine of them were homozygous for the *aae13-1* mutation. Seven of these nine plants were indistinguishable from wild-type plants grown under the same conditions (Figure 7B). *aae13-1* BjMCS plants were also fully fertile and produced abundant seed. RT-PCR analysis using BjMCS gene-specific primers showed that the complemented *aae13-1* mutant contained BjMCS transcripts, whereas the untransformed wild-type control did not (Figure 7A).

Additional phenotypic characterization was performed on T2 progeny derived from one complemented line, T1-11. Twenty-seven progeny of this plant were genotyped by PCR as *aae13-1* homozygous mutant plants, among which 20 were wild-type in appearance, while seven were small and sickly rosettes. PCR analysis using BjMCS gene-specific primers revealed that all 20 normal-looking plants contained the BjMCS transgene, whereas none of the seven small plants did. The ratio between small and normal T2 plants (7:20) is a good fit to the 1:3 hypothesis for a single insertion of the transgene that complements the *aae13-1* mutant phenotype.

We also constructed a vector containing an *AAE13* cDNA under control of the *AAE13* promoter and a BASTA resistance gene and transformed this into *AAE13/aae13-1* hemizygous plants to complement the *aae13-1* mutation. Transgenic T1 plants transformed with ProAAE13:AAE13 cDNA were selected

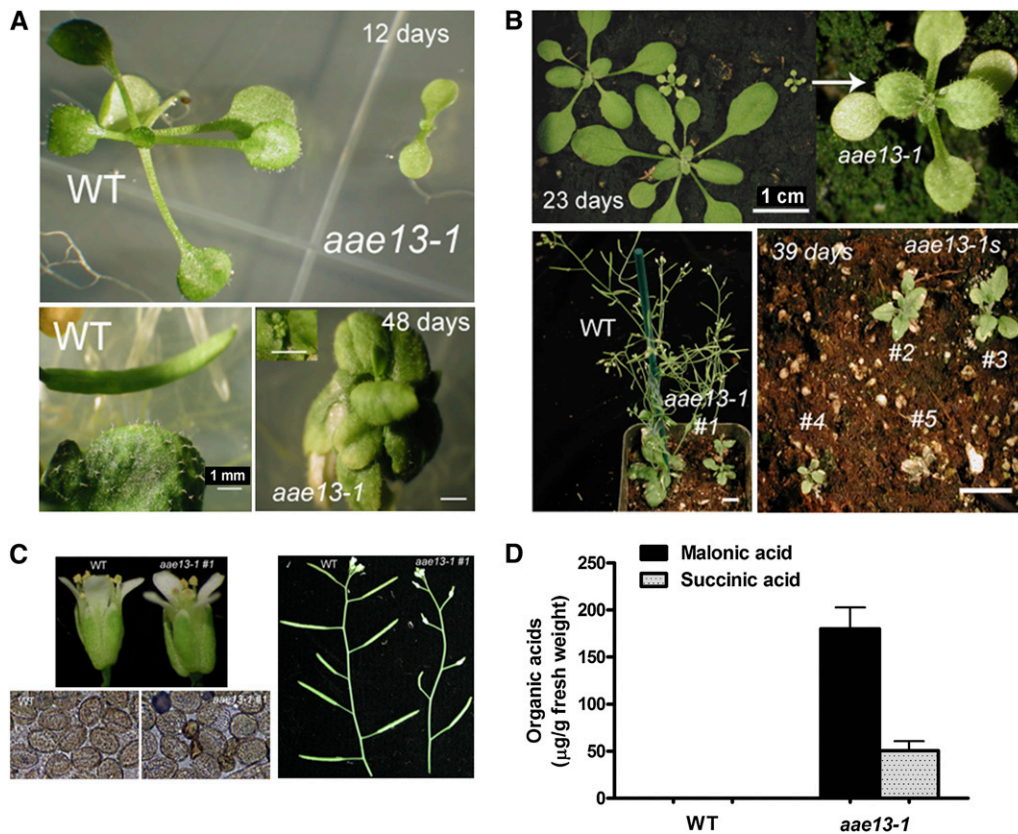


Figure 6. Phenotypic Characterization of the *aae13-1* Mutant.

(A) Phenotypes of wild-type (WT) and *aae13-1* plants after 12 d (top) and 48 d (bottom) growth on agar medium supplemented with 1% Suc. For *aae13-1* at 48 d, the inset shows an alternative view of the apical region.

(B) Severely reduced growth and development of *aae13-1* plants on soil after 23 d (top) and 39 d (bottom). The plant *aae13-1* #1 is one of the few that matured and eventually set seed.

(C) Comparison of flowers, pollen, and siliques of *aae13-1* #1 (right in each panel) and the wild type.

(D) Concentrations of malonic acid and succinic acid measured in 12-d-old seedlings of the wild type and *aae13-1*. In the wild type, concentrations were below the detection limit of ~ 2 $\mu\text{g/g}$ fresh weight. Data are means \pm SD of three independent measurements.

on BASTA-treated soil and genotyped for *AAE13* and *aae13-1* alleles, as well as for the presence of the *AAE13* transgene, using the primers P1, P2, and LBA1. As shown in Figures 7C and 7D, two out of 28 normal-looking T1 plants analyzed (plants #15 and #21 lacking the endogenous *AAE13* allele) were homozygous *aae13-1* mutant plants. These two mutant plants also contained the *AAE13* transgene from which the gene-specific primers P1 and P2 amplified a 0.5-kb fragment. This fragment from the cDNA can be distinguished from the 0.4-kb fragment amplified with the primers LBA1 and P2 from the genomic DNA of hemizygous or homozygous mutant plants, which is also observed for plants #15 and #21.

These results indicate that expression of either the bacterial malonyl-CoA synthetase or native *AAE13* can complement the *aae13-1* mutant phenotype. We can conclude that the extensive growth and reproductive defects of mutant plants are caused by the loss of malonyl-CoA synthetase activity rather than any additional mutation(s) in the *aae13-1* line.

Plants Overexpressing *AAE13* Show Increased Sensitivity to Exogenous Malonate

Our conclusion that the malonyl-CoA synthetase encoded by *AAE13* is required to remove toxic malonic acid suggested that overexpression of *AAE13* might provide increased protection from exogenous malonate. To test this possibility, we generated transgenic *Arabidopsis* in which an *AAE13* cDNA is expressed under control of the 35S promoter. Three independent transgenic lines were identified as having malonyl-CoA synthetase activities at least 50-fold higher than the low activities found in wild-type tissues (Figure 3B). One of these lines, Pro35S:*AAE13*#6, is described here, and the two additional lines (#71 and #84) provided similar results in all respects. As shown in Figure 8A, homozygous plants from line Pro35S:*AAE13*#6 were indistinguishable from the wild type in growth and appearance during normal culture. Enzymatic assays of tissue extracts (Figure 8B) revealed high activities of malonyl-CoA synthetase

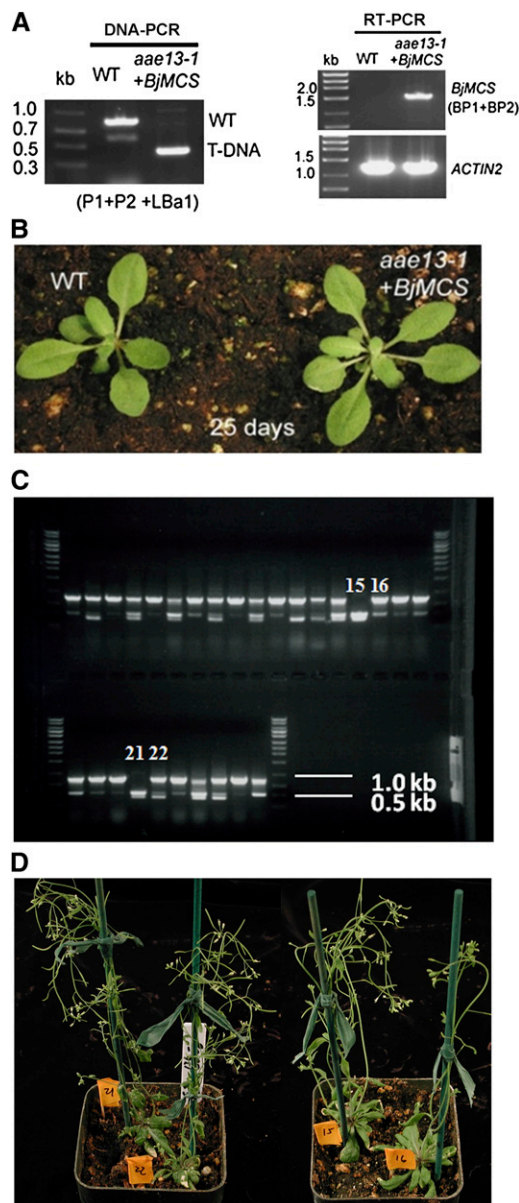


Figure 7. Complementation of the *aae13-1* Mutant.

(A) Identification of *aae13-1* plants expressing the malonyl-CoA synthetase from *B. japonicum* under control of the *AAE13* promoter (construct p*BjMCS*). Genomic PCR (left panel) with primers P1, P2, and LBa1 confirm absence of the wild-type (WT) allele. RT-PCR (right panel) with primers BP1+BP2, specific for the coding sequence in *BjMCS*, confirm expression of the bacterial gene. Three independent complemented lines were analyzed, with similar results.

(B) The *BjMCS* transgene restores growth of the *aae13-1* mutant (right) to the wild type.

(C) Genotyping of T1 progeny of an *AAE13/aae13-1* heterozygous plant transformed with a *AAE13* cDNA under control of the *AAE13* promoter. Healthy, BASTA-resistant T1 plants were genotyped using primers P1, P2, and LBa1. Absence of the band at 0.9 kb, derived from the endogenous *AAE13* allele, indicates that plants #15 and #21 are *aae13-1* homozygotes. The band at 0.5 kb is derived from the cDNA sequence

in both leaves (31.3 nmol/min/mg fresh weight) and flowers (28.6 nmol/min/mg fresh weight). This constitutive high expression reduced malonic acid in the flowers to undetectable levels (Figure 8C), but this had no measureable effect on floral development or plant fertility.

To test whether overexpression of malonyl-CoA synthetase can protect plants from exogenous malonate, we grew Pro35S:*AAE13*#6 plants and wild-type controls on agar plates using the protocol previously employed with wild-type plants (Figure 4A). Surprisingly, the plants overexpressing *AAE13* were more susceptible than the wild type (Figure 8D). Compared with wild-type seedlings growing on the same plates, Pro35S:*AAE13*#6 seedlings were healthy on 1 mM malonate and had only a minimal reduction in growth on 2 mM malonate. However, on 5 mM malonate, a concentration that induces only a modest effect on wild-type seedlings, both root and shoot growth of Pro35S:*AAE13*#6 seedlings are severely reduced (Figure 8D). While constitutive overexpression of malonyl-CoA synthetase is benign under normal growth conditions, providing exogenous malonate to the plants severely compromises their growth. One possible explanation for these results is that high activity of malonyl-CoA synthetase in the presence of 5 mM exogenous malonate disrupts metabolism through increased flux through pathways using malonyl-CoA or possibly through sequestration of CoA. However, these possibilities appear not to have a direct bearing on the physiological role of *AAE13* in wild-type plants.

DISCUSSION

Our characterization of the recombinant, His-tagged *AAE13* protein indicates that the *AAE13* gene product is an active and specific malonyl-CoA synthetase. Other dicarboxylic acids and fatty acids of different chain lengths were not recognized as substrates, except for a low activity measured with 2-methylmalonic acid (Table 1). This substrate specificity is noteworthy because many of the proteins in the 44-member *Arabidopsis* *AAE* superfamily (Shockey et al., 2003) exhibit confusingly broad substrate specificities during *in vitro* assays (Shockey et al., 2003; Schneider et al., 2005), and efforts to identify the physiological substrate(s) by this means have not always been successful. In the case of *AAE13*, the results of our investigation of the *aae13* mutant support the conclusion that it acts as a malonyl-CoA synthetase *in vivo*. Mutant seedlings accumulate malonic acid (Figure 6D), indicating a defect in catabolism of this compound. In addition, the strong, pleiotropic phenotype of the mutant was successfully complemented by expression of a previously characterized malonyl-CoA synthetase from *B. japonicum* (Figures 7A and 7B).

Malonyl-CoA synthetase activity has been described from both plants and mammals (Hatch and Stumpf, 1962; Koeppen

of the transgene. (The 0.4-kb band derived from the *aae13-1* allele migrates slightly below this.)

(D) Growth and development of homozygous *aae13-1* plants carrying the transgene (plants #15 and #21) are similar to wild-type (plant #16) and heterozygous (plant #22) siblings.

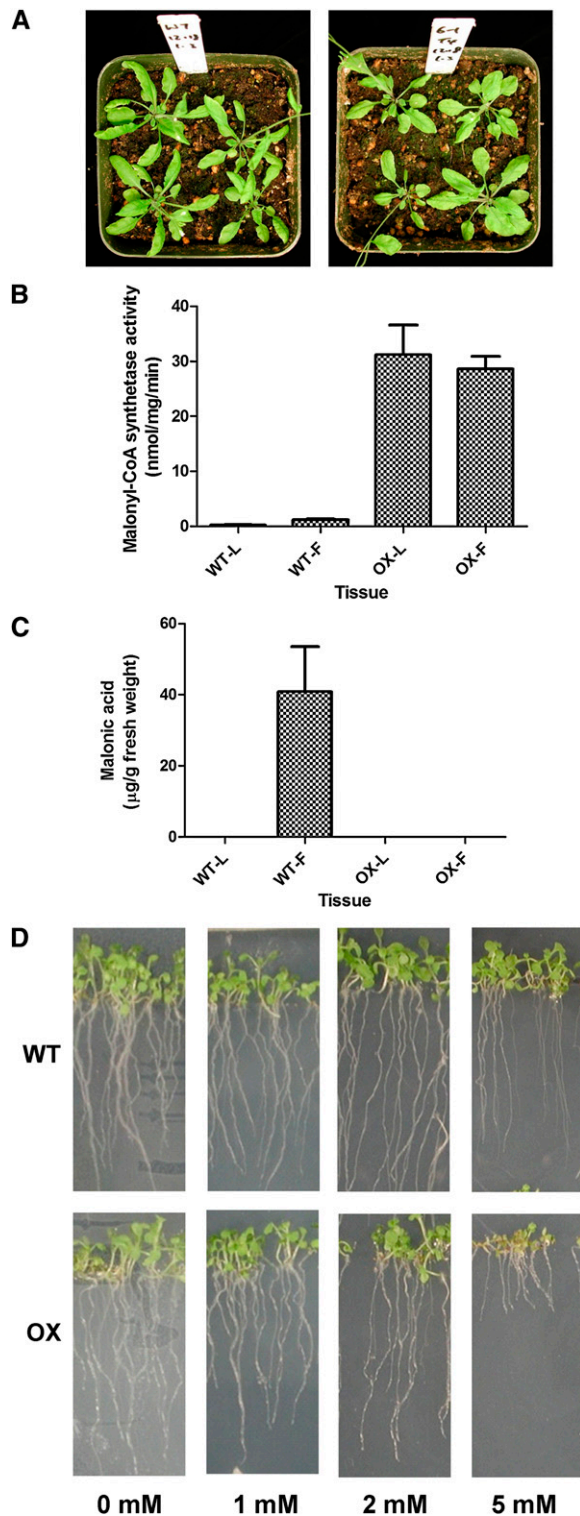


Figure 8. Characterization of Plants Overexpressing AAE13.

(A) Phenotype of wild-type (left) and plants homozygous for the Pro35S:AAE13 transgene (line #6; right). **(B)** and **(C)** Malonyl-CoA synthetase activity **(B)** and malonic acid content **(C)** in rosette (L) and flower (F) tissues of 6-week-old wild-type (WT) and

et al., 1974; Gueguen et al., 2000). The human genome encodes 26 demonstrated or putative acyl-CoA synthetases, but a gene encoding malonyl-CoA synthetase has not previously been identified. When we used AAE13 as a query sequence to search the human protein database using the BLASTP search engine at the National Center for Biotechnology Information (blast.ncbi.nlm.nih.gov), the ACSF3 protein was identified as the most closely related sequence, with 39% identity, 55% similarity, and a high BLAST score (sum probability e^{-103}). The next-highest scoring protein, ACSM3 (acyl-CoA synthetase medium-chain family member 3) showed only 34% identity, 44% similarity, and a sum probability value of e^{-33} . ACSF3 has previously been proposed to be a very-long-chain acyl-CoA synthetase on the basis of a somewhat modest increase in the activity of COS1 cells expressing an ACSF3 cDNA relative to cells transfected with an empty vector as control (Watkins et al., 2007). On the basis of our biochemical characterization of partially purified, recombinant His-tagged ACSF3 (see Supplemental Figure 1 online) and the results of sequence analysis (Figure 2), we propose that ACSF3 is an ortholog of AAE13 (and *matB*) and encodes a malonyl-CoA synthetase. Considering the severe consequences of the *aae13* mutation for plant growth, development, and reproduction, it would be interesting to know the phenotype of knockout mice mutated in ACSF3. However, as of December, 2010, the resource center for knockout mouse lines (www.knockoutmouse.org) did not have such a line available.

The T-DNA insertion that caused the *aae13-1* mutation is located in the 12th exon of the gene and prevents transcription of 246 bp of the wild-type coding sequence. RT-PCR provided evidence for a chimeric mRNA that would potentially be translated into a truncated protein containing 23 amino acids encoded by the T-DNA insert (Figure 5). However, the sequence of 82 amino acids at the C terminus of AAE13 is highly similar to other malonyl-CoA synthetases (Figure 2) and constitutes part of the LuxE domain that is characteristic of AAE proteins and related AMP binding proteins (Shockey et al., 2003). For this reason, it is likely that the *aae13-1* mutant is null. Our assays of recombinant protein from *E. coli* expressing a cDNA encoding the *aae13-1* mutant protein detected no malonyl-CoA synthetase activity. Given the detection limit of our assay, this indicates that the mutant protein has no more than 2% of the wild-type activity.

Compared with wild-type controls, the growth, development, and reproduction of the *aae13-1* mutant are severely affected at many stages of the life cycle, both on agar medium supplemented with 1% Suc and on soil (Figure 6). Under all the growth conditions tested, we observed a stochastic aspect to plant survival, suggesting that plants were compromised to a point where relatively small environmental differences determined whether they lived or died. The small proportion of plants that did flower produced few seeds. The severe pleiotropic phenotype of the *aae13-1* mutant, together with its complementation

Pro35S:AAE13 transgenic (OX) plants. Data are means \pm SD ($n = 3$).

(D) Wild-type and Pro35S:AAE13 (OX) seedlings grown on agar plates supplemented with different concentrations of malonic acid. The pictures were taken 7 d after germination.

by cDNAs for either *AAE13* or the *B. japonicum matB* gene under control of the *AAE13* promoter (Figure 7), indicate that the malonyl-CoA synthetase encoded by *AAE13* is essential for normal growth and reproduction in plants.

It is unlikely that the *aae13-1* phenotype is caused by a deficiency in malonyl-CoA. Both biochemical and genetic evidence indicate that the predominant synthesis of malonyl-CoA in plants occurs via acetyl-CoA carboxylase (Konishi and Sasaki, 1994; Baud et al., 2003, 2004). The cytoplasmic form of this enzyme is encoded in *Arabidopsis* by *ACC1*, and the malonyl-CoA produced is used for the synthesis of sphingolipids, cuticular waxes, flavonoids, and other compounds essential to plant function. *acc1* mutants are defective in embryo development, and, although the seeds germinate, seedling development is arrested before any expansion of the cotyledons occurs (Baud et al., 2003, 2004). Interestingly, this *acc1* phenotype could be partially relieved by addition of malonic acid to the agar growth medium (Baud et al., 2004). This result indicates that malonyl-CoA synthetase can provide an alternative source of malonyl-CoA to support seedling establishment but that endogenous production of malonate in germinating seeds is not sufficient to provide this essential substrate in the amounts required for seedling growth and establishment. The localization of our *AAE13*-GFP fusion protein to the nucleus as well as the cytoplasm raises the possibility that *AAE13* may be necessary for malonyl-CoA synthesis in the nucleus. Alternatively, despite the reproducibility of nuclear localization in our experiments, it remains possible that the results are artifactual. In this respect, it is noteworthy that all aspects of the *aae13* mutant phenotype are complemented by expression of the bacterial MatB malonyl-CoA synthetase, which would certainly not be expected to enter the nucleus. We conclude that the essential function of the *AAE13* enzyme is likely to be as a cytoplasmic malonyl-CoA synthetase.

We consider it most likely that the *AAE13* enzyme is required to metabolize malonic acid and prevent it from accumulating to toxic levels in cells and tissues of the plant. Malonic acid is a competitive inhibitor of succinate dehydrogenase, a key enzyme of the tricarboxylic acid cycle (Quastel and Wooldridge, 1928; Greene and Greenamyre, 1995), so disruption of intermediary metabolism in cells provides a plausible mechanism underlying the severe pleiotropic phenotype of the *aae13-1* mutant shown in Figure 6. In wild-type plants, we detected malonic acid in concentrations of 33 ± 7 $\mu\text{g/g}$ fresh weight in flower tissue (Figure 3D), but in all other tissues tested, the concentrations were below the detection limit of our measurements (~ 2 $\mu\text{g/g}$ fresh weight). When wild-type plants were grown on increasing concentrations of exogenous malonic acid, seedling growth was first visibly reduced at 5 mM malonic acid in the medium (Figure 4A). The shoots of these plants contained 250 $\mu\text{g/g}$ fresh weight malonic acid and 70 $\mu\text{g/g}$ fresh weight succinic acid (Figure 4C). Significantly, similar concentrations of both malonic acid (180 $\mu\text{g/g}$ fresh weight) and succinic acid (50 $\mu\text{g/g}$ fresh weight) were found in seedlings of the *aae13-1* mutant germinated in the absence of malonic acid (Figure 6D). Thus, two different routes to increasing malonic acid concentrations in seedlings both compromise plant growth and are associated with the accumulation of succinic acid, which indicates a likely inhibition of succinate

dehydrogenase and, thus, flux through the tricarboxylic acid cycle.

There are a number of pathways that could contribute to malonic acid production in plant cells. These include the oxidative decarboxylation of oxaloacetate (de Vellis et al., 1963), hydrolysis of malonyl-CoA (Stumpf and Burris, 1981), and possibly the degradation of pyrimidines (Hayaishi and Kornberg, 1952). Malonic acid can also be formed from malondialdehyde by aldehyde dehydrogenase. Malondialdehyde is derived from peroxidation of polyunsaturated fatty acids, and its production is stimulated by oxidative stress, osmotic stress, and ABA treatment (Hung and Kao, 2004; Kotchoni et al., 2006; Farmer and Davoine, 2007; Mène-Saffrané et al., 2007). In this respect, it is noteworthy that transcriptional profiling data available from the *Arabidopsis* Gene Expression Atlas (Schmid et al., 2005) indicate that expression of *AAE13* is induced by both osmotic stress and ABA (see Supplemental Figure 3 online). Malondialdehyde itself is toxic (Esterbauer et al., 1991; Farmer and Davoine, 2007), and considerable indirect evidence indicates that it is detoxified by oxidation to malonate (Sunkar et al., 2003; Kotchoni et al., 2006; Rodrigues et al., 2006; Huang et al., 2008; Shin et al., 2009).

Regardless of the source or sources of malonate, our results indicate that malonyl-CoA synthetase encoded by *AAE13* is required for its detoxification. Interestingly, acetyl-CoA synthetase performs a similar detoxification role in the plastid. Acetyl-CoA for fatty acid synthesis is derived mainly from pyruvate via pyruvate dehydrogenase, but acetyl-CoA synthetase participates in the removal of acetate formed from toxic acetaldehyde during fermentation (Oliver et al., 2009). The phenotypes of the *aae13* mutants and our other results reported here indicate that the production and metabolism of malonic acid are important, neglected pathways in plant biochemistry.

METHODS

Plant Materials and Growth Conditions

Arabidopsis thaliana (ecotype Columbia) was grown on Murashige and Skoog basal medium (MS salts; Sigma-Aldrich) containing 0.8% (w/v) Bacto agar (Becton-Dickinson) and 1% Suc or in potting soil in a chamber (photosynthetic photon flux density 150 μmol of photons $\text{m}^{-2} \text{s}^{-1}$, 22°C, 8-h night). A T-DNA mutant line, *aae13-1* (SALK_083785) for *AAE13*, was obtained from the ABRC (Ohio State University, Columbus, OH). The primers P1 (5'-TCCCAGTTTGTAAATGGCAATG-3'), P2 (5'-GAGCAAGCTTGCTTTAGCCC-3'), and LBa1 (5'-TGGTTCACGTAGTGGCCATCG-3') were used for the genotyping of T-DNA insertion mutant. The chimeric transcript was amplified using P3 (5'-CACCATGGAAGTGT-TAAAGCAGCT-3') and P6 (5'-GGTGAAGGGCAATCAGCTGTTGCC-3') primers from first-strand cDNA prepared from *aae13-1* mutant plant.

Chemicals

Tartronic acid (2-hydroxymalonic acid) was purchased from Alfa Aesar. Unless otherwise noted, other chemicals were purchased from Sigma-Aldrich Chemical Company.

AAE13 Phylogeny

Members of the *AAE13* superfamily and its related sequences were identified from the HomoloGene database at the National Center for

Biotechnology Information (<http://www.ncbi.nlm.nih.gov/homologene/>). Amino acid sequences were aligned using AlignX program in Vector NTI (Informax).

Expression and Purification of Recombinant AAE13 and ACSF3

Full-length *AAE13* was amplified by PCR from cDNA prepared from 200 ng of flower total RNA with the *AAE13*-specific primers AAE13F (5'-CACCATGGAAGTGTAAAGCAGCT-3') as the forward primer and AAE13R (5'-TTATTCTTGATTTCCAGAGA-3') as the reverse primer, respectively. PCR products were cloned into pENTR/D-TOPO vector (Invitrogen) to make pENTR-AAE13 cDNA and completely sequenced. Then, the DNA fragment was transferred into Gateway bacterial expression vector pDEST17 using the Gateway LR Clonase recombination reaction (Invitrogen). pDEST17 contains an N-terminal 6xHis-tag. The resulting plasmid pDEST17-AAE13 was transformed into *Escherichia coli* strain BL21AI-competent cells (Invitrogen). An overnight culture (2 mL) was inoculated into 40 mL of Luria-Bertani medium supplemented with 100 µg/mL ampicillin. Bacteria were grown at 37°C in a shaker at 250 rpm for 3 h to a cell density of $\sim 0.5 A_{600}$, and then the culture was cooled down to 18°C and 0.2% (w/v) L-arabinose was added to the culture. The induced culture was incubated for 16 h at 18°C. Cells were collected by centrifugation and frozen using liquid nitrogen.

A full-length human *ACSF3* cDNA clone was PCR amplified from pcDNA3-ACSF3 vector (Watkins et al., 2007) with the primer set of *NotI* (5'-AAAGCGCCGCATGCTGCCCATGTGGTGCTC-3') as the forward primer and *XhoI* (5'-GTGCTCGAGTGAGGGGTGGAAGTGCCTGATGAGCGCT-3') as the reverse primer, respectively. The resulting PCR product was cleaved with *NotI* and *XhoI* and cloned into the corresponding restriction sites of pRMG-nMAL (Thines et al., 2007) to make the MBP-ACSF3-His6 fusion plasmid. The resulting plasmid was transformed into *E. coli* strain BL21AI-competent cells. An overnight culture (2 mL) was inoculated into 40 mL of Luria-Bertani medium supplemented with 100 µg/mL ampicillin. Bacteria were grown at 37°C in a shaker at 250 rpm for 3 h to a cell density of $\sim 0.5 A_{600}$, and then 0.2% (w/v) L-arabinose was added to the culture. The induced culture was incubated for 3 h at 37°C. Cells were collected by centrifugation and frozen using liquid nitrogen.

Purification of the His-tagged proteins was performed at 4°C using the Qproteome bacterial protein preparation kit from Qiagen according to the instructions from the manufacturer. Briefly, frozen cells were thawed on ice for 15 min and resuspended in native lysis buffer supplemented with lysozyme and Benzonase nuclease. After incubation on ice for 30 min with gentle shaking, the lysate was centrifuged at 20,000g for 20 min at 4°C to pellet the cellular debris. The resulting supernatant was collected and loaded onto a Ni-nitriloacetic acid agarose column (Invitrogen) equilibrated with binding buffer (5 mM imidazole, 500 mM NaCl, and 20 mM Tris-HCl, pH 7.9). After the column was washed with binding buffer and washing buffer (30 mM imidazole, 500 mM NaCl, and 20 mM Tris-HCl, pH 7.9), His-tagged proteins were eluted with elution buffer (250 mM imidazole, 500 mM NaCl, and 20 mM Tris-HCl, pH 7.9). Imidazole was removed from the protein samples with a 5-mL spin column packed with Sephadex G-25 (Amersham Biosciences) and equilibrated with 100 mM Tris-HCl buffer, pH 7.5. Protein concentrations were determined by the Bradford method (Bradford, 1976) using BSA as a standard. The relative purity of recombinant protein was assessed by SDS-PAGE and staining of gels with Coomassie Brilliant Blue R 250.

Measurement of Acyl-CoA Synthetase Activity

Acyl-CoA synthetase activities of recombinant AAE13 were measured using the coupled enzyme assay (Ziegler et al., 1987; Koo et al., 2006). Briefly, reaction mixtures (800 µL) contained 0.1 M Tris-HCl, pH 7.5, 2 mM

DTT, 5 mM ATP, 10 mM MgCl₂, 0.5 mM CoA, 0.4 mM NADH, 200 µM carboxylic acid substrate, 1 mM phosphoenolpyruvate, and 10 units each of myokinase, pyruvate kinase, and lactate dehydrogenase. The reaction was initiated by adding ~ 5 µg of purified enzyme. Oxidation of NADH was monitored at 340 nm with a Beckman DU530 spectrophotometer.

Alternatively, an HPLC-based method was developed for the measurement of acyl-CoA synthetase activity, which allows the use of crude extracts as enzyme source and buffers with different pH values. Typically, reaction mixtures (800 µL) contained 0.1 M Tris-HCl, pH 7.5, 2 mM DTT, 5 mM ATP, 10 mM MgCl₂, 0.5 mM CoA, and 200 µM carboxylic acid substrate. The reaction was initiated by adding 5 µg of purified AAE13 protein or 50 to 100 µL of crude enzyme preparation from *Arabidopsis* tissues. Assays were stopped after 10 min by addition of 40 µL acetic acid. The solution was filtered through a 0.45-µm filter prior to analysis by HPLC. HPLC was performed with an Alliance 2695 HPLC system (Waters) using a SymmetryShield C18 column (Waters; 150 × 3.9 mm) and a 2996 photodiode array detector. The mobile phase consisted of solvent A (0.1% trifluoroacetic acid) and solvent B (acetonitrile). The gradient elution procedure was as follows: 0 to 5 min, 0% of B; 5 to 35 min, a linear gradient from 0 to 60% of B; 35 to 38 min, 60% of B; 38 to 40 min, 0% of B. The flow rate was 1.0 mL/min. The diode array detector collected data in the 200- to 400-nm range. For detection and quantification of substrate and products, peak areas were measured at 257 nm.

For crude enzyme extract preparation, frozen *Arabidopsis* tissues were ground in 1.5-mL Eppendorf tubes with a pestle in the presence of liquid nitrogen and then homogenized in ~ 0.5 mL of 100 mM Tris-HCl, pH 7.5, containing 1 mM EDTA, 1% (v/v) 2-mercaptoethanol, and 0.1 mM phenylmethylsulfonyl fluoride. Homogenates were centrifuged at 14,000 rpm for 10 min at 4°C, and the supernatants were used as the enzyme source. Protein concentrations were determined by the Bradford method (Bradford, 1976) using BSA as a standard.

Two buffer systems were used to test the effect of pH on malonyl-CoA synthetase activity: 200 mM potassium phosphate, pH 6.0, 6.5, 7.0, and 7.5; and 100 mM Tris-HCl, pH 7.5, 8.0, 8.5, and 9.0.

Metabolic Profiling of Water-Soluble Constituents in Plant Samples by GC-MS

The extraction of water-soluble metabolites from plant tissues and the subsequent analysis by GC-MS were based on the published protocol with some modification (Broeckling et al., 2005). Briefly, ~ 50 mg fresh leaves or 30 mg flowers were ground in a 1.5-mL Eppendorf tube with a pestle in the presence of liquid nitrogen and then 0.5 mL of chloroform was added. The sample was thoroughly vortexed and incubated for 60 min at 50°C. Then, 0.5 mL of water containing 80 µg/mL ribitol was added to the chloroform. The sample was vortexed and incubated for a second 60-min period. After cooling to room temperature, the biphasic solvent system was centrifuged at 2900g for 30 min to separate the layers. Then, 0.35 mL of the polar layer was collected, transferred to a new vial, and dried in a Speed-Vac concentrator.

Dried polar extracts were methoximated with 100 µL of MOX reagent (2% methoxyamine-HCl in pyridine; Pierce Biotechnology) at 50°C for 30 min. Metabolites were then derivatized with 100 µL of *N*-methyl-*N*-trimethylsilyl-trifluoroacetamide/1% trimethylchlorosilane (Pierce Biotechnology) for 30 min at 50°C. The sample was subsequently transferred to a 200-µL glass insert and analyzed by GC-MS.

Next, 1.0 µL of the solution was injected at a 15:1 split ratio onto a HP 6890 GC equipped with a 30m Rtx-5 Sil MS column (Restek; 0.25-mm ID and 0.25-µm film thickness) coupled to a HP 5973 MS. The injection port and transfer arm were held at 280°C. Separation was achieved with a temperature program of 80°C for 3 min and then ramped at 5°C/min to 315°C and held for 6 min. The MS source was held at 230°C and the quadrupole at 150°C and scanned from mass-to-charge ratio of 50 to 800.

Mutant Complementation

The *AAE13* promoter was amplified with the primers AAE13pro-N (5'-CACCTTTGGAGACAGTCTCTGAAA-3') and AAE13pro-C (5'-GAGTGAACCAGACTGTGAAG-3'). Amplicates were cloned into pENTR/D-TOPO vector (Invitrogen) to make pENTR-AAE13P construct and completely sequenced.

To make AAE13P-AAE13-cDNA fusion construct, primers AAE13P5 (5'-CACCTTTGGAGACAGTCTCTGAAAAGTTTCAAGCA-3') and LINK-AAE13PC (5'-TTCTGAAAAAGCTGCTTTAAACACTTCCATGAGTGAAC-CAGACTGTGAAGCTGCAACATT-3') were used to amplify the *AAE13* promoter fragment and primers LINK-AAE13C (5'-AATGTTGCAGCTTACAGTCTGGTTCAGTCTCATGGAAGTGTAAAGCAGCTTTTTTCAGAA-3') and AAE13C-TER (5'-TTATTCTTGATTTCCAGAGATTTCTTTAG-3') were used to amplify the *AAE13* cDNA fragment, respectively. The two PCR-derived fragments were purified and pooled, and the fusion fragment was obtained through PCR reaction using the primers AAE13P5 and AAE13C-TER. The BjMCS construct was made by PCR in a similar way.

We transformed the ProAAE13:AAE13 or BjMCS constructs into *AAE13/aae13-1* heterozygous plants through the floral dip method (Clough and Bent, 1998). T1 transgenics were selected for BASTA resistance in soil. Twenty-eight and 48 Basta-resistant plants were randomly chosen for genotyping the presence or absence of the *AAE13* wild-type allele in ProAAE13:AAE13 and BjMCS constructs, respectively.

Subcellular Localization

Full-length *AAE13* minus stop codon was amplified from cDNA with AAE13F forward primer and the reverse primer 5'-TTCTTGATTTCCA-GAGA-3'. Amplicates were cloned into pENTR TOPO and then subcloned by Gateway LR recombination into the vector pB7FWG2, generating in-frame fusions with the N terminus of enhanced GFP driven by the cauliflower mosaic virus (CaMV) 35S promoter (Karimi et al., 2002) to generate a Pro35S:AAE13-GFP construct. A full-length *AAE13* cDNA (with stop codon) in the pENTR TOPO vector was subcloned by Gateway LR recombination into the vector p2FGW7, generating in-frame fusions with the C terminus of enhanced GFP driven by the CaMV 35S promoter to generate a Pro35S:GFP-AAE13 construct.

Pro35S:AAE13-GFP, Pro35S:GFP-AAE13, and Pro35S:GFP (control) constructs were delivered into protoplasts prepared from leaf tissue of 3-week-old wild-type *Arabidopsis* by polyethylene glycol-mediated transfection (Jin et al., 2001). Protoplasts were incubated under lights at room temperature for 14 h before images were taken with a Zeiss LSM 710 confocal microscope. The GFP fluorescence was excited by an argon laser (488 nm) and was collected from 505 to 525 nm. Chloroplast autofluorescence was detected between 664 and 696 nm with excitation at 488 nm.

Generation of Pro35S:AAE13 Plants

AAE13 cDNA fragment in pENTR TOPO was transferred by LR recombination cloning (Invitrogen) into the pB2GW7 destination vector (Karimi et al., 2002) for expression under control of the CaMV 35S promoter. Constructs were introduced into *Agrobacterium tumefaciens* strain GV3101. Wild-type *Arabidopsis* plants were transformed by the floral dip method (Clough and Bent, 1998). T1 transgenics were selected for BASTA resistance (120 mg/L) in soil and screened for malonyl-CoA synthetase activity by HPLC. In the T2 generation, three homozygous, high-expression lines were identified, Pro35S:AAE13#6, #71, and #84, and used for experimental comparisons to the wild type.

Accession Numbers

Sequence data from this article can be found in the Arabidopsis Genome Initiative or GenBank/EMBL databases under the following accession

numbers: AAE13, At3g16170, AAP03025.1; *Bradyrhizobium japonicum* Bj MCS, AAF28840.1; Hs ACSF3, AAH28399.1; *Rhizobium leguminosarum* MCS, ACC83455.

Supplemental Data

The following materials are available in the online version of this article.

Supplemental Figure 1. ACSF3 Is a Malonyl-CoA Synthetase.

Supplemental Figure 2. Subcellular Localization of AAE13.

Supplemental Figure 3. Induction of the Expression of *AAE13* by Osmotic Stress and ABA.

Supplemental Table 1. Expression Profile of Human ACSF3 from Analysis of EST Counts.

ACKNOWLEDGMENTS

We thank Yu Sam Kim (Yonsei University) for providing the *R. japonicum* *matB* gene and Paul Watkins (Johns Hopkins University School of Medicine) for the gift of human ACSF3 cDNA in pcDNA3 vector. This work was supported by the National Science Foundation (Grant MCB-0420199) and by the Agricultural Research Center at Washington State University.

Received April 6, 2011; revised April 6, 2011; accepted May 16, 2011; published June 3, 2011.

REFERENCES

- An, J.H., and Kim, Y.S. (1998). A gene cluster encoding malonyl-CoA decarboxylase (MatA), malonyl-CoA synthetase (MatB) and a putative dicarboxylate carrier protein (MatC) in *Rhizobium trifolii*—Cloning, sequencing, and expression of the enzymes in *Escherichia coli*. *Eur. J. Biochem.* **257**: 395–402.
- Baud, S., Bellec, Y., Miquel, M., Bellini, C., Caboche, M., Lepiniec, L., Faure, J.D., and Rochat, C. (2004). *gurke* and *pasticcino3* mutants affected in embryo development are impaired in acetyl-CoA carboxylase. *EMBO Rep.* **5**: 515–520.
- Baud, S., Guyon, V., Kronenberger, J., Wuillème, S., Miquel, M., Caboche, M., Lepiniec, L., and Rochat, C. (2003). Multifunctional acetyl-CoA carboxylase 1 is essential for very long chain fatty acid elongation and embryo development in *Arabidopsis*. *Plant J.* **33**: 75–86.
- Begley, T.P., Kinsland, C., and Strauss, E. (2001). The biosynthesis of coenzyme A in bacteria. *Vitam. Horm.* **61**: 157–171.
- Bellin, S.A., and Smeby, R.R. (1958). Malonic acid in green and cured American and oriental tobaccos. *Arch. Biochem. Biophys.* **75**: 1–5.
- Bentley, L.E. (1952). Occurrence of malonic acid in plants. *Nature* **170**: 847–848.
- Bradford, M.M. (1976). A rapid and sensitive method for the quantitation of microgram quantities of protein utilizing the principle of protein-dye binding. *Anal. Biochem.* **72**: 248–254.
- Broeckling, C.D., Huhman, D.V., Farag, M.A., Smith, J.T., May, G.D., Mendes, P., Dixon, R.A., and Sumner, L.W. (2005). Metabolic profiling of *Medicago truncatula* cell cultures reveals the effects of biotic and abiotic elicitors on metabolism. *J. Exp. Bot.* **56**: 323–336.
- Clough, S.J., and Bent, A.F. (1998). Floral dip: A simplified method for *Agrobacterium*-mediated transformation of *Arabidopsis thaliana*. *Plant J.* **16**: 735–743.
- de Vellis, J., Shannon, L.M., and Lew, J.Y. (1963). Malonic acid

- biosynthesis in bush bean roots. I. Evidence for oxaloacetate as immediate precursor. *Plant Physiol.* **38**: 686–690.
- Dimroth, P., and Hilbi, H.** (1997). Enzymic and genetic basis for bacterial growth on malonate. *Mol. Microbiol.* **25**: 3–10.
- Emanuelsson, O., Nielsen, H., Brunak, S., and von Heijne, G.** (2000). Predicting subcellular localization of proteins based on their N-terminal amino acid sequence. *J. Mol. Biol.* **300**: 1005–1016.
- Esterbauer, H., Schaur, R.J., and Zollner, H.** (1991). Chemistry and biochemistry of 4-hydroxynonenal, malonaldehyde and related aldehydes. *Free Radic. Biol. Med.* **11**: 81–128.
- Farmer, E.E., and Davoine, C.** (2007). Reactive electrophile species. *Curr. Opin. Plant Biol.* **10**: 380–386.
- Fatland, B.L., Nikolau, B.J., and Wurtele, E.S.** (2005). Reverse genetic characterization of cytosolic acetyl-CoA generation by ATP-citrate lyase in *Arabidopsis*. *Plant Cell* **17**: 182–203.
- Greene, J.G., and Greenamyre, J.T.** (1995). Characterization of the excitotoxic potential of the reversible succinate dehydrogenase inhibitor malonate. *J. Neurochem.* **64**: 430–436.
- Groot, P.H., Scholte, H.R., and Hülsmann, W.C.** (1976). Fatty acid activation: Specificity, localization, and function. *Adv. Lipid Res.* **14**: 75–126.
- Gueguen, V., Macherel, D., Jaquinod, M., Douce, R., and Bourguignon, J.** (2000). Fatty acid and lipoic acid biosynthesis in higher plant mitochondria. *J. Biol. Chem.* **275**: 5016–5025.
- Hatch, M.D., and Stumpf, P.K.** (1962). Fat metabolism in higher plants. XVII. Metabolism of malonic acid & its alpha-substituted derivatives in plants. *Plant Physiol.* **37**: 121–126.
- Hayashi, O.** (1955). Enzymatic decarboxylation of malonic acid. *J. Biol. Chem.* **215**: 125–136.
- Hayashi, O., and Kornberg, A.** (1952). Metabolism of cytosine, thymine, uracil, and barbituric acid by bacterial enzymes. *J. Biol. Chem.* **197**: 717–732.
- Horton, P., Park, K.J., Ohbayashi, T., and Nakai, K.** (2006). Protein subcellular localization prediction with WoLF PSORT. In 4th Asia-Pacific Bioinformatics Conference (APBC2006), T. Jiang, U.C. Yang, Y.P.P. Chen, and L. Wong, eds (London: Imperial College Press), pp. 39–48.
- Huang, W., Ma, X., Wang, Q., Gao, Y., Xue, Y., Niu, X., Yu, G., and Liu, Y.** (2008). Significant improvement of stress tolerance in tobacco plants by overexpressing a stress-responsive aldehyde dehydrogenase gene from maize (*Zea mays*). *Plant Mol. Biol.* **68**: 451–463.
- Hung, K.T., and Kao, C.H.** (2004). Hydrogen peroxide is necessary for abscisic acid-induced senescence of rice leaves. *J. Plant Physiol.* **161**: 1347–1357.
- Jin, J.B., Kim, Y.A., Kim, S.J., Lee, S.H., Kim, D.H., Cheong, G.W., and Hwang, I.** (2001). A new dynamin-like protein, ADL6, is involved in trafficking from the trans-Golgi network to the central vacuole in *Arabidopsis*. *Plant Cell* **13**: 1511–1526.
- Karimi, M., Inzé, D., and Depicker, A.** (2002). GATEWAY vectors for Agrobacterium-mediated plant transformation. *Trends Plant Sci.* **7**: 193–195.
- Kim, Y.S.** (2002). Malonate metabolism: Biochemistry, molecular biology, physiology, and industrial application. *J. Biochem. Mol. Biol.* **35**: 443–451.
- Kim, Y.S., and Bang, S.K.** (1985). Malonyl coenzyme A synthetase. Purification and properties. *J. Biol. Chem.* **260**: 5098–5104.
- Kim, Y.S., and Chae, H.Z.** (1991). Purification and properties of malonyl-CoA synthetase from *Rhizobium japonicum*. *Biochem. J.* **273**: 511–516.
- Kim, Y.S., Kwon, S.J., and Kang, S.W.** (1993). Malonyl-CoA synthetase from *Rhizobium trifolii*: Purification, properties, and the immunological comparison with those from *Bradyrhizobium japonicum* and *Pseudomonas fluorescens*. *Korean Biochem. J.* **26**: 176–183.
- Koeppe, A.H., Mitzen, E.J., and Ammoumi, A.A.** (1974). Malonate metabolism in rat brain mitochondria. *Biochemistry* **13**: 3589–3595.
- Konishi, T., and Sasaki, Y.** (1994). Compartmentalization of two forms of acetyl-CoA carboxylase in plants and the origin of their tolerance toward herbicides. *Proc. Natl. Acad. Sci. USA* **91**: 3598–3601.
- Koo, A.J., Chung, H.S., Kobayashi, Y., and Howe, G.A.** (2006). Identification of a peroxisomal acyl-activating enzyme involved in the biosynthesis of jasmonic acid in *Arabidopsis*. *J. Biol. Chem.* **281**: 33511–33520.
- Koo, H.M., and Kim, Y.S.** (2000). Identification of active-site residues in *Bradyrhizobium japonicum* malonyl-coenzyme A synthetase. *Arch. Biochem. Biophys.* **378**: 167–174.
- Kotchoni, S.O., Kuhns, C., Ditzer, A., Kirch, H.H., and Bartels, D.** (2006). Over-expression of different aldehyde dehydrogenase genes in *Arabidopsis thaliana* confers tolerance to abiotic stress and protects plants against lipid peroxidation and oxidative stress. *Plant Cell Environ.* **29**: 1033–1048.
- Li, J., and Copeland, L.** (2000). Role of malonate in chickpeas. *Phytochemistry* **54**: 585–589.
- Liu, Y., Su, L.Y., and Yang, S.F.** (1984). Stereoselectivity of 1-aminocyclopropanecarboxylate malonyltransferase toward stereoisomers of 1-amino-2-ethylcyclopropanecarboxylic acid. *Arch. Biochem. Biophys.* **235**: 319–325.
- Mène-Saffrané, L., Davoine, C., Stolz, S., Majcherczyk, P., and Farmer, E.E.** (2007). Genetic removal of tri-unsaturated fatty acids suppresses developmental and molecular phenotypes of an *Arabidopsis* tocopherol-deficient mutant. Whole-body mapping of malondialdehyde pools in a complex eukaryote. *J. Biol. Chem.* **282**: 35749–35756.
- Mirecka, E.A., Rudolph, R., and Hey, T.** (2006). Expression and purification of His-tagged HPV16 E7 protein active in pRB binding. *Protein Expr. Purif.* **48**: 281–291.
- Mitzen, E.J., and Koeppe, A.H.** (1984). Malonate, malonyl-coenzyme A, and acetyl-coenzyme A in developing rat brain. *J. Neurochem.* **43**: 499–506.
- Nelson, E.K., and Hasselbring, H.** (1931). Some organic acids of wheat plants. *J. Am. Chem. Soc.* **53**: 1040–1043.
- Ohlrogge, J., and Browse, J.** (1995). Lipid biosynthesis. *Plant Cell* **7**: 957–970.
- Oliver, D.J., Nikolau, B.J., and Wurtele, E.S.** (2009). Acetyl-CoA-Life at the metabolic nexus. *Plant Sci.* **176**: 597–601.
- Peer, W.A., Brown, D.E., Tague, B.W., Muday, G.K., Taiz, L., and Murphy, A.S.** (2001). Flavonoid accumulation patterns of transparent testa mutants of *Arabidopsis*. *Plant Physiol.* **126**: 536–548.
- Quastel, J.H., and Wooldridge, W.R.** (1928). Some properties of the dehydrogenating enzymes of bacteria. *Biochem. J.* **22**: 689–702.
- Rodrigues, S.M., Andrade, M.O., Gomes, A.P., Damatta, F.M., Baracat-Pereira, M.C., and Fontes, E.P.** (2006). *Arabidopsis* and tobacco plants ectopically expressing the soybean antiquitin-like ALDH7 gene display enhanced tolerance to drought, salinity, and oxidative stress. *J. Exp. Bot.* **57**: 1909–1918.
- Schmid, M., Davison, T.S., Henz, S.R., Pape, U.J., Demar, M., Vingron, M., Schölkopf, B., Weigel, D., and Lohmann, J.U.** (2005). A gene expression map of *Arabidopsis thaliana* development. *Nat. Genet.* **37**: 501–506.
- Schneider, K., Kienow, L., Schmelzer, E., Colby, T., Bartsch, M., Miersch, O., Wasternack, C., Kombrink, E., and Stuible, H.P.** (2005). A new type of peroxisomal acyl-coenzyme A synthetase from *Arabidopsis thaliana* has the catalytic capacity to activate biosynthetic precursors of jasmonic acid. *J. Biol. Chem.* **280**: 13962–13972.
- Shin, J.H., Kim, S.R., and An, G.** (2009). Rice aldehyde dehydrogenase7 is needed for seed maturation and viability. *Plant Physiol.* **149**: 905–915.
- Shockey, J.M., Fulda, M.S., and Browse, J.** (2003). *Arabidopsis* contains a large superfamily of acyl-activating enzymes. *Phylogenetic*

- and biochemical analysis reveals a new class of acyl-coenzyme A synthetases. *Plant Physiol.* **132**: 1065–1076.
- Stumpf, D.K., and Burris, R.H.** (1981). Biosynthesis of malonate in roots of soybean seedlings. *Plant Physiol.* **68**: 992–995.
- Sunkar, R., Bartels, D., and Kirch, H.H.** (2003). Overexpression of a stress-inducible aldehyde dehydrogenase gene from *Arabidopsis thaliana* in transgenic plants improves stress tolerance. *Plant J.* **35**: 452–464.
- Taguchi, G., Ubukata, T., Nozue, H., Kobayashi, Y., Takahi, M., Yamamoto, H., and Hayashida, N.** (2010). Malonylation is a key reaction in the metabolism of xenobiotic phenolic glucosides in *Arabidopsis* and tobacco. *Plant J.* **63**: 1031–1041.
- Thines, B., Katsir, L., Melotto, M., Niu, Y., Mandaokar, A., Liu, G., Nomura, K., He, S.Y., Howe, G.A., and Browse, J.** (2007). JAZ repressor proteins are targets of the SCF(COI1) complex during jasmonate signalling. *Nature* **448**: 661–665.
- Turner, W.A., and Hartman, A.M.** (1925). The non-volatile organic acid of alfalfa. *J. Am. Chem. Soc.* **47**: 2044–2047.
- Vickery, H.B.** (1959). The metabolism of the organic acids of tobacco leaves. XVI. Effect of culture of excised leaves in solutions of malonate. *J. Biol. Chem.* **234**: 1363–1368.
- Watkins, P.A., Maiguel, D., Jia, Z., and Pevsner, J.** (2007). Evidence for 26 distinct acyl-coenzyme A synthetase genes in the human genome. *J. Lipid Res.* **48**: 2736–2750.
- Ziegler, K., Braun, K., Böckler, A., and Fuchs, G.** (1987). Studies on the anaerobic degradation of benzoic acid and 2-aminobenzoic acid by a denitrifying *Pseudomonas* strain. *Arch. Microbiol.* **149**: 62–63.